

## Coherent Backscattering of Light in a Quasi-Two-Dimensional System

Isaac Freund, Michael Rosenbluh, Richard Berkovits, and Moshe Kaveh

*Department of Physics, Bar-Ilan University, Ramat-Gan, Israel*

(Received 2 February 1988)

We present the first experiments on coherent backscattering of light in a quasi-two-dimensional system, and find reasonably good agreement with a theory that accounts for small departures from strictly two dimensions. The photon density near the sample boundaries is obtained from the angular dependence of the diffusely transmitted and reflected light, and is found to be in substantial agreement with the two-dimensional photon diffusion equation. Prospects for observing the logarithmic correction to the optical transmission of a two-dimensional system appear encouraging.

PACS numbers: 71.55.Jv, 42.20.-y

Multiple scattering of light, the effects of localization, and the optical Anderson transition,<sup>1,2</sup> are areas of intense current interest.<sup>3-26</sup> Weak localization, the precursor to strong localization, manifests itself, *inter alia*, in the form of a coherent, back-directed peak superimposed upon light diffusely scattered from a random medium.<sup>3-6</sup> This striking phenomenon has recently been the subject of intensive study in three-dimensional systems.<sup>3-9</sup> Here, we report the first observations of coherent backscattering of light from a two-dimensional (2D) system. Using a spatially anisotropic optical diffusion constant, we incorporate deviations from 2D into the theory of coherent backscattering from a finite system,<sup>10</sup> and find reasonably good agreement with our data. From Milne theory<sup>27</sup> and the angular dependence of the diffuse scattering we obtain, for the first time, the spatial variation of the photon density near the boundaries of a 2D system, and find substantial agreement with the two-dimensional photon diffusion equation. Our present samples have an effective dimensionality  $d = 2 + \epsilon = 2.05$ , and a transport mean free path approximately 60 times the wavelength  $\lambda = 0.63 \mu\text{m}$ . Under these conditions the localization length is enormously greater than the sample thickness  $s$ , and the effects of strong localization are unobservable. We estimate, however, that it is feasible to obtain  $l/\lambda \sim 2$ , and  $\epsilon \sim 6 \times 10^{-3}$ , which would permit the first observations of the weak-localization logarithmic correction<sup>25</sup> to the optical transmission predicted for a 2D system.<sup>10</sup>

For a system to behave optically as a two-dimensional one, it is necessary that the random walk of the multiply scattered photon be confined to a plane. Although this may be achieved by use of a thin sample between totally reflecting walls, it is exceedingly difficult to fabricate the requisite broad-band, lossless mirrors. Recognizing that it is the random walk of the photon which must be 2D, rather than the sample geometry, we have obtained an optically 2D system using randomly spaced, long parallel rods. In our case the rod length is over  $1000\lambda$ , so that the momentum transfer parallel to the rod axis approaches zero, and a photon injected perpendicular to

the rods executes a planar random walk.

Our samples were composed of microscopic ( $\sim 5200 \text{ \AA}$ ) fibrils of the natural protein collagen supported by a complex mucopolysaccharide matrix. Details on sample preparation and characterization have been given in another context.<sup>28</sup> Using Mie theory and the known system parameters,<sup>28</sup> we calculate transport mean free paths of  $40 \mu\text{m}$  for light polarized parallel to the rods ( $z$  axis), and  $85 \mu\text{m}$  for light polarized in the perpendicular  $xy$  plane. The rods were aligned by tension. In our best sample the mean angular deviation from perfect parallelism was estimated to be  $\phi \approx 2^\circ$ , which leads to  $\epsilon \approx (2\langle \sin^2 \phi \rangle)^{1/2} = 0.05$ , and an effective dimensionality  $d = 2.05$ .

In Fig. 1 we display far-field photographs of the coherent backscattering. Figure 1(a) was obtained with a stationary sample and shows the expected sample-specific optical fluctuations<sup>8,9,12,13</sup> which mask the backscattering peak. In Fig. 1(b), the sample was oscillated about its long axis, thereby performing an ensemble average which permits the coherent backscattering to be seen as a bright vertical line superimposed upon a band

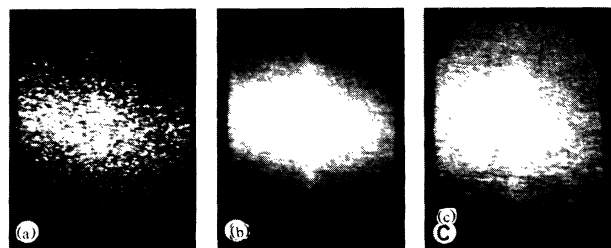


FIG. 1. Backscattering patterns. (a) Stationary sample displaying large-amplitude optical fluctuations which mask the coherent backscattering. (b) Oscillating sample resulting in ensemble averaging which reveals the coherent backscattering as a bright vertical line. (c) Sample under reduced tension leading to significant departure from 2D. The line of coherent backscattering is diffused and fades out vertically into the background.

of diffuse scattering centered on the equator. For perfectly aligned rods, i.e., perfect 2D, both the coherent and diffuse scattering would be constrained to the equator, so that the length of the line of coherent scattering and the height of the diffuse band are due to system imperfections. Since the rod tilts are small, however, substantial coherence is maintained in the vertical direction, and the line of coherent backscattering extends almost all the way through the diffuse band. In Fig. 1(c) the tension on the sample was partly relaxed, thereby disordering the system and increasing its departure from 2D. This leads to an increase in the height of the diffuse band and a relative shortening of the coherent line, which may be seen to fade out vertically.

$$I(q_y, q_x, s) = F(q_z) [1 - a/s + (1/2qa) \{ \coth(qs) [1 - \cosh(2qa)] + \sinh(2qa) \}], \quad (1)$$

where  $F(q_z)$  is the square of the rod form factor averaged over  $\phi$ ,  $a = (1 + \Delta)l$ , and

$$q = [(D_y/D_x)q_y^2 + (D_z/D_x)q_z^2]^{1/2},$$

so that the contours of constant backscattering intensity are ellipses. Continuous photon injection all along the incident beam path leads to a complex expression which differs significantly from the above only at large  $q$  values for which our signal is lost in noise.  $\Delta$  is determined by the boundary conditions, and, as discussed later, an appropriate value for 2D is  $\Delta = 0.8$

When  $D_x = D_y = D_{xy} \gg D_z$ , a finite sample exhibits 2D behavior if  $D_{xy}/D_z > (s/l)^2$ , while for larger  $s$  the photon breaks out of the  $xy$  plane and a crossover to 3D behavior occurs. In general, the departure from 2D may be characterized by  $\epsilon = (D_z/D_{xy})^{1/2}$ . Important predictions of Eq. (2) are the following: (i) scanning  $q_y$  along the equator ( $q_z = 0$ ) yields the usual peak shape, height, and width.<sup>4-9</sup> (ii) Scanning  $q_y$  at constant nonzero  $q_z$  yields a reduced peak height and increased peak width. (iii) Along the meridian ( $q_y = 0$ ), the width of a  $q_z$  scan, and hence the length of the line of coherent backscattering in Fig. 1, decreases rapidly with  $D_z$ .

If we define  $D_z$  via the mean square distance along  $z$  traveled in time  $t$ ,  $\langle z^2 \rangle = D_z t$ ,  $D_z$  may be written in terms of the rod tilt angle  $\phi$ , as  $D_z = 2D_{xy} \langle \sin^2 \phi \rangle$ . As  $D_z \rightarrow D_{xy}$ , the system becomes the usual isotropic three-dimensional one, the height of the diffuse band expands to fill the whole back (and front) hemisphere, the bright line in Fig. 1 shrinks to a point, and the contours of constant coherent intensity become concentric circles. The initial stages of this transformation are displayed qualitatively in Fig. 1.

In Fig. 2 we display  $q_y$  scans obtained with a vertically oriented slit centered on the equator. In comparing the data with Eq. (2), the height of this slit was accounted for by appropriate averaging over  $q_z$ . A fit to the data yielded  $D_x/D_{xy} = 0.002$ , corresponding to  $\epsilon = 0.05$ , and a mean tilt angle for the rods  $\phi \approx 2^\circ$ , which is consistent

Sample imperfections cause the multiply scattered photon to slowly diffuse out of the  $xy$  plane, leading to a mapping of our problem onto the anisotropic diffusion equation

$$\left[ \frac{\partial^2}{\partial x^2} + \frac{D_y}{D_x} \frac{\partial^2}{\partial y^2} + \frac{D_z}{D_x} \frac{\partial^2}{\partial z^2} \right] \rho = \frac{1}{D_x} \frac{\partial \rho}{\partial t}, \quad (1)$$

where  $\rho$  is the photon density, and the  $D$ 's are the diffusion constants along the three principal axes. For a slab of thickness  $s$  along the  $x$  axis with photon injection at  $x = l$ , we obtain in the usual way<sup>6,7,10,11</sup> the coherent backscattering as a function of momentum transfer  $q_y, q_z$ ,

$$(2)$$

with the height of the diffuse band. In performing this fit we also found it necessary to include a 12%  $q$ -independent, "single scattering" term similar to that found in all 3D experiments.<sup>4-9</sup> A  $q_y$  scan along the upper third of the coherent line in Fig. 1(b) yielded a

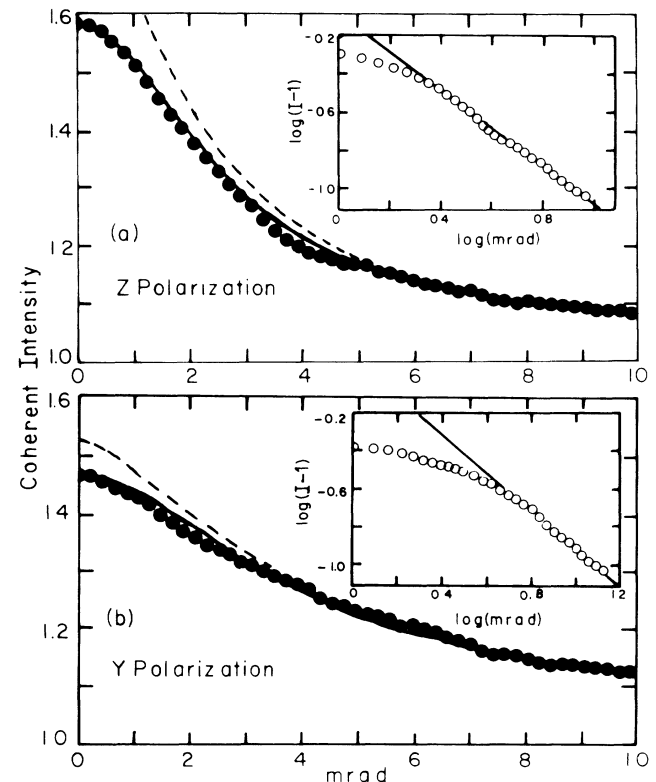


FIG. 2. Equatorial line scans of coherent backscattering vs scattering angle in mrad. In the main figures, the solid lines are fits to Eq. (2) with dimensionality  $d=2.05$ , while the dashed lines are for  $d=2$ . The slope of the straight lines in the insets is  $-1$ , corresponding to the asymptotic falloff of net coherent intensity  $I-1$  with the inverse of the scattering angle.

peak-to-background ratio for  $z$ -polarized light of 1.33, in reasonably good agreement with the calculated value of 1.36. In accord with the 2D nature of the sample, no measurable depolarization of the scattered light was detected.

The mean free path for  $y$  polarization is twice that for  $z$  polarization, so that the curve in Fig. 2(b) should be half as wide as the curve in Fig. 2(a), instead of being twice as wide. We believe this discrepancy is most likely due to the very long mean free path and the finite spot size of the laser beam (0.5 mm). This effect may be approximately included by use of a value for  $s$  in Eq. (2) somewhat smaller than the true value (0.23 mm), since both finite beam size and finite sample thickness broaden the curve by cutting off long light paths.<sup>4,7-11</sup> We found that reducing  $s$  by 20% was sufficient to yield a reasonably good fit also for the  $y$ -polarization data. At larger  $q$ , only short light paths are important, and as shown in the insets to Fig. 2, the predicted  $1/q$  falloff is found.

The value of  $\Delta$  which enters Eq. (2) is determined by the boundary conditions for the photon diffusion equation, and depends upon dimensionality. In 3D, the diffusion equation yields  $\Delta = \frac{2}{3}$ , while the Milne equation gives  $\Delta = 0.7104$ .<sup>27</sup> In 1D, the diffusion equation and the Milne equation both give  $\Delta = 1$ . In 2D, the diffusion equation gives  $\Delta = \pi/4$ , while preliminary analysis of the Milne equation suggests  $\Delta = 0.8$ , which is the value employed here. If we expand the photon density a little inside the boundary as

$$\rho(x) = \sum_{n=0}^{\infty} \rho_n x^n, \quad (3a)$$

where  $x$  measures the distance from the boundary in units of  $l$ , the angular dependence of the diffuse background scattering may be obtained from Milne theory as

$$I_B(\theta) = I_0 \sum_{n=0}^{\infty} \rho_n n! \cos^{n+1} \theta, \quad (3b)$$

where  $\theta$  is measured from the surface normal. Thus, a measurement of  $I_B$  yields, for the first time, the spatial variation of  $\rho$  near the boundaries of a two-dimensional system.

For a source located deep inside the random medium far from the boundary, the diffusion equation yields  $\rho_0/\rho_1 = \Delta$ , while all other terms vanish. This corresponds approximately to the case of the diffusely transmitted light, whose angular dependence is thus predicted to be  $I_B(\theta) = I_0(\Delta \cos \theta + \cos^2 \theta)$ . In Fig. 3(a) we plot the measured data for both  $z$  and  $y$  polarizations. The calculated curves are least-squares fits to a function of the form  $I_B(\theta) = A \cos \theta + B \cos^2 \theta$ , which provides an excellent description of the data. Within the small standard deviations of the parameters, we find for both polarizations  $B = 1.05A$ , implying  $\Delta = 0.95$ , so that overall, the level of agreement with theory is reasonable.

Near the entrance face of the sample, the local rate of

photon loss via diffusion is approximately balanced by continuous injection along the beam path, and a more-or-less flat photon density is expected, leading to  $I_B(\theta) = I_0 \cos \theta$ . The experimental data are shown in Fig. 3(b). Here the straight lines are least-squares fits to  $I_B(\theta) = A + B \cos \theta$ , where a nonzero value for  $A$  provides a sensitive indicator of any curvature. For both polarizations, we find that within less than 1 standard deviation  $A = 0$ , implying a very flat photon density distribution near the entrance face, as shown in the inset to the figure. This distribution, although in general agreement with expectation, is rather flatter than predicted by a detailed calculation. Nonetheless, our experiments generally confirm the essential validity and applicability of the two-dimensional photon diffusion equation and its associated boundary conditions.

For the sample to be effectively 2D, one requires

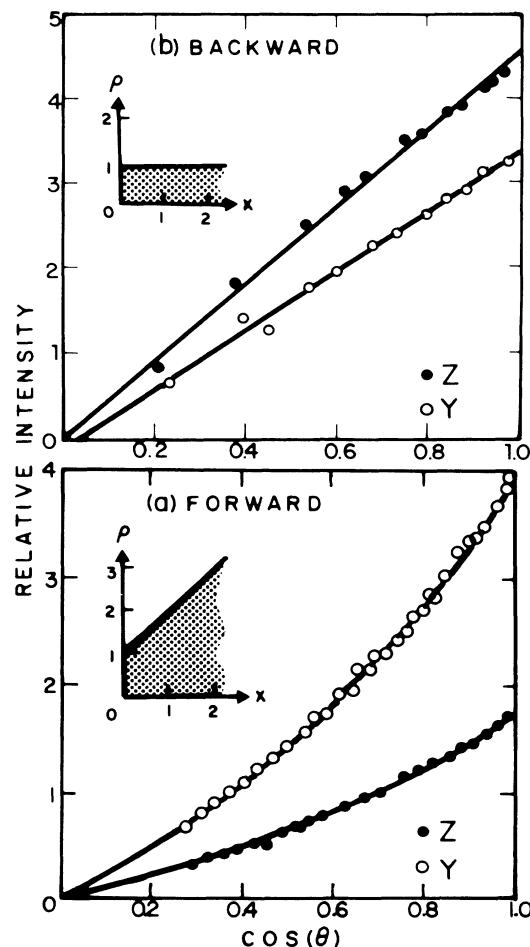


FIG. 3. Angular dependence in (a) transmission, and (b) reflection of the diffuse scattering for  $z$ -polarized (filled circles), and  $y$ -polarized (open circles) light vs the cosine of the scattering angle. The fitted curves are discussed in the text. Insets: The photon density in the vicinity of the boundaries as derived from the scattering data.

$\epsilon < l/2s$ . When this is satisfied, we can expect to be able to observe the logarithmic correction<sup>25</sup> to the optical transmission  $(\lambda/2\pi^2l)\ln(s/l)$  predicted<sup>10</sup> for a 2D system. Fine fibers similar to those used here, but with no supporting matrix, are calculated to yield  $l = 2\lambda$ . A similar mean free path is also obtained for fine channels etched through a block of transparent material. For such samples a measurable 10% correction to the transmission is predicted for a 100- $\mu\text{m}$ -thick sample if  $\epsilon < 0.006$ , corresponding to a mean effective tilt angle of the rods (or channels)  $\phi < 0.2^\circ$ . It appears feasible to meet these conditions, leading to the possibility of the first observations of this unique effect of weak localization of light in two dimensions.

We are pleased to acknowledge the kind interest and perceptive comments of Sir Nevill Mott, useful discussions with B. Shapiro, and the assistance of I. Edrei. We are also pleased to acknowledge the support of the Israel Academy of Sciences.

<sup>1</sup>S. John, Phys. Rev. Lett. **53**, 2169 (1984), and **58**, 2486 (1987).

<sup>2</sup>P. W. Anderson, Philos. Mag. **B 52**, 505 (1985).

<sup>3</sup>Y. Kuga and A. Ishimaru, J. Opt. Soc. Am. **A 1**, 831 (1984); L. Tsang and A. Ishimaru, J. Opt. Soc. Am. **A 2**, 2187 (1985).

<sup>4</sup>M. P. van Albada and A. Lagendijk, Phys. Rev. Lett. **55**, 2692 (1985); M. P. van Albada, M. B. van der Mark, and A. Lagendijk, Phys. Rev. Lett. **58**, 361 (1987); A. Lagendijk, M. P. van Albada, and M. B. van der Mark, Physica (Amsterdam) **140A**, 183 (1986).

<sup>5</sup>P. E. Wolf and G. Maret, Phys. Rev. Lett. **55**, 2696 (1985).

<sup>6</sup>E. Akkermans, P. E. Wolf, and R. Maynard, Phys. Rev. Lett. **56**, 1471 (1986).

<sup>7</sup>M. J. Stephen, Phys. Rev. Lett. **56**, 1809 (1986); M. J. Stephen and G. Cwilich, Phys. Rev. **B 34**, 7564 (1986).

<sup>8</sup>S. Etemad, R. Thompson, and M. J. Andrejco, Phys. Rev. Lett. **57**, 575 (1986); S. Etemad, R. Thompson, M. J. Andrejco, S. John, and F. C. MacKintosh, Phys. Rev. Lett. **59**, 1420 (1987).

<sup>9</sup>M. Kaveh, M. Rosenbluh, I. Edrei, and I. Freund, Phys. Rev. Lett. **57**, 2049 (1986); M. Rosenbluh, I. Edrei, M. Kaveh, and I. Freund, Phys. Rev. **A 35**, 4458 (1987).

<sup>10</sup>R. Berkovits and M. Kaveh, J. Phys. **C 20**, L181 (1987), and Phys. Rev. **B 36**, 9322 (1988); M. Kaveh, Philos. Mag. **B 56**, 693 (1987).

<sup>11</sup>F. C. Mackintosh and S. John, Phys. Rev. **B 37**, 1884 (1988).

<sup>12</sup>B. Shapiro, Phys. Rev. Lett. **57**, 2168 (1986).

<sup>13</sup>M. J. Stephen and G. Cwilich, Phys. Rev. Lett. **59**, 285 (1987).

<sup>14</sup>G. H. Watson, Jr., P. A. Fleury, and S. L. McCall, Phys. Rev. Lett. **58**, 945 (1987).

<sup>15</sup>A. Genack, Phys. Rev. Lett. **58**, 2043 (1987).

<sup>16</sup>A. A. Golebentsev, Zh. Eksp. Teor. Fiz. **86**, 47 (1984) [JETP Lett. **30**, 228 (1984)].

<sup>17</sup>G. Maret and P. Wolf, Z. Phys. **B 65**, 409 (1987).

<sup>18</sup>M. Rosenbluh, M. Hoshen, I. Freund, and M. Kaveh, Phys. Rev. Lett. **58**, 2754 (1987); M. Kaveh, M. Rosenbluh, and I. Freund, Nature (London) **326**, 778 (1987); I. Freund, M. Rosenbluh, and M. Kaveh, Phys. Rev. Lett. **60**, 1130 (1988).

<sup>19</sup>P. Sheng and Z. Zhang, Phys. Rev. Lett. **57**, 1879 (1987).

<sup>20</sup>C. A. Condat and T. R. Kirkpatrick, Phys. Rev. Lett. **58**, 226 (1987).

<sup>21</sup>K. Arya, Z. B. Su, and J. L. Birman, Phys. Rev. Lett. **57**, 2725 (1986).

<sup>22</sup>W. Chen and D. L. Mills, Phys. Rev. Lett. **58**, 160 (1987).

<sup>23</sup>M. Kohmoto, B. Sutherland, and K. Iguchi, Phys. Rev. Lett. **58**, 2436 (1987).

<sup>24</sup>J. E. Sipe, P. Sheng, B. S. White, and M. H. Cohen, Phys. Rev. Lett. **60**, 108 (1988).

<sup>25</sup>E. Abrahams, P. W. Anderson, P. W. Licciardello, and T. V. Ramakrishnan, Phys. Rev. Lett. **42**, 673 (1979).

<sup>26</sup>For reviews on electron localization, see G. Bergman, Phys. Rep. **107**, 1 (1984); M. Pepper, Contemp. Phys. **26**, 257 (1985); P. A. Lee and T. V. Ramakrishnan, Rev. Mod. Phys. **57**, 287 (1985); N. F. Mott and M. Kaveh, Adv. Phys. **34**, 329 (1985).

<sup>27</sup>P. M. Morse and H. Feshbach, *Methods of Theoretical Physics* (McGraw-Hill, New York, 1953).

<sup>28</sup>I. Freund, M. Deutsch, and A. Sprecher, Biophys. **J. 50**, 693 (1986).

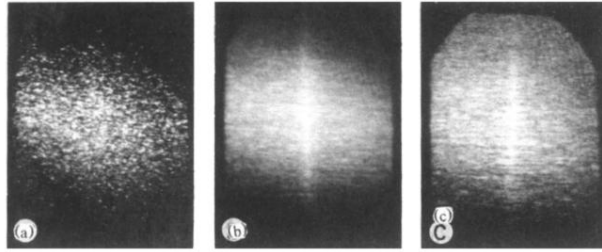


FIG. 1. Backscattering patterns. (a) Stationary sample displaying large-amplitude optical fluctuations which mask the coherent backscattering. (b) Oscillating sample resulting in ensemble averaging which reveals the coherent backscattering as a bright vertical line. (c) Sample under reduced tension leading to significant departure from 2D. The line of coherent backscattering is diffused and fades out vertically into the background.

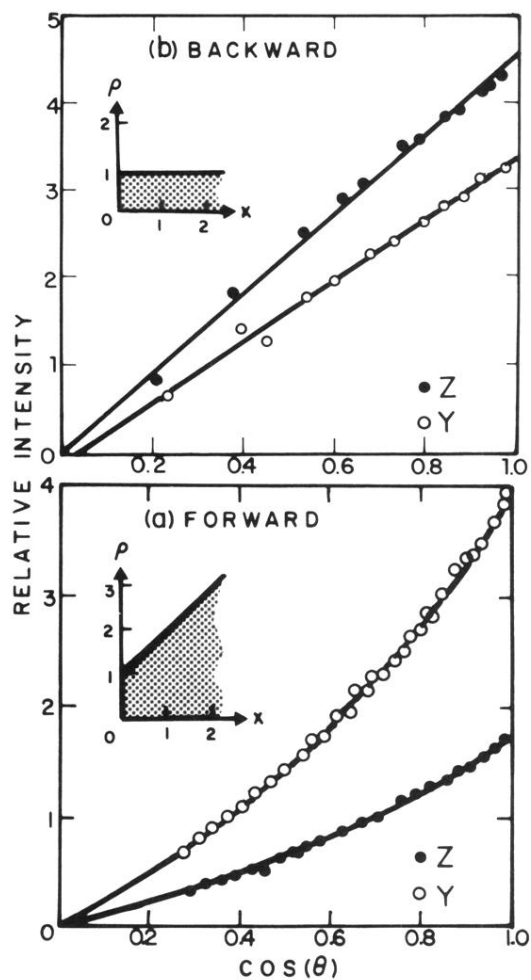


FIG. 3. Angular dependence in (a) transmission, and (b) reflection of the diffuse scattering for z-polarized (filled circles), and y-polarized (open circles) light vs the cosine of the scattering angle. The fitted curves are discussed in the text. Insets: The photon density in the vicinity of the boundaries as derived from the scattering data.